

Total Intensity and Quasi-elastic Light Scattering Applications in Microbiology

By Stephen E. Harding

UNIVERSITY OF NOTTINGHAM, DEPARTMENT OF APPLIED
BIOCHEMISTRY AND FOOD SCIENCE, SUTTON BONINGTON, LE12 5RD,
U.K.

1. INTRODUCTION

The previous chapters in this volume have considered the advances in laser light scattering theory and methodology followed by specific applications to systems of biological macromolecules. In this first chapter on "large" macromolecular assemblies we will survey some of the many recent applications of laser light scattering to problems in microbiology and focus on some of the work that we have been specifically involved with on viral and bacterial systems. The review element of this Chapter is intended to supplement an earlier article from this laboratory¹. The reader is also referred to a more general review by Bloomfield² which includes a consideration of quasi-elastic light scattering (QLS) applications in virology and to the study of microbial motility, and an earlier article by Wyatt³ which considers total intensity light scattering (TILS) applications in bacteriology.

Laser light scattering applications in microbiology can be broken down conceptually into two parts: 1. studies on the macromolecular components of microbes: this has essentially been covered earlier in this volume: many of the macromolecular systems considered there are microbial in origin; 2. studies on whole micro-organisms: this will be considered here.

Studies on "whole" microbes offer certain advantages and certain disadvantages as far as laser light scattering techniques are concerned. The advantages include (i) the greater signal to noise

ratio (that is to say also the so-called "dust problem" is not as severe⁴); (ii) the correspondingly smaller concentrations generally required to give a sufficient signal; (iii) since the wavelength of the incident laser light can be of the same order as the maximum dimension of the microbe (Fig. 1), internal structural information can, in principle, be obtained from the nature of the "resonances" in the angular scattered intensity envelopes³.

The relatively large size - compared to macromolecular systems - of microbial scatterers also brings problems, namely that we are on the limits, and in many cases go beyond them, of the applicability of the relatively simple "Rayleigh-Gans-Debye" representations of the scattering data. These criteria, already considered by Wyatt⁵ in this volume are summarised by the two equations:

$$\left| \frac{n}{n_0} - 1 \right| \ll 1 \quad (1)$$

$$(4\pi na/\lambda_0)|(n/n_0)| \ll 1 \quad (2)$$

a is the maximum dimension of the scatterer, n , n_0 the refractive indices of scatterer and surrounding medium respectively and λ_0 the wavelength of the incident light. These criteria are usually satisfied for smaller microbes, such as most viruses, and the highly useful limiting case or "Zimm plot" can also be applied. They can also be satisfied for larger micro-organisms - for example vegetative bacterial cells suspended in an aqueous media where $\ln n_0$ is very small - although because of the resonances, the Zimm plot and related representations become inapplicable. For the highly dehydrated and refractile bacterial spores - particularly air-borne particles - the criteria are not satisfied, and for this case, interpretation of the scattering records can be rendered opaque because of the complexity of the mathematical representations ("Lorenz-Mie" theory) involved⁶. A further problem for the larger or denser microbes is that sedimentation phenomena can also obscure this interpretation. Nonetheless, if one allows for these reservations laser light scattering methods, both total intensity, or quasi-elastic, can provide powerful - and unlike for example electron microscopy, non-destructive - probes into the structure and dynamics of microbial systems, as we will consider now. In this consideration, details of the theory and instrumentation behind both the total intensity ("static") and quasi-elastic ("dynamic") light scattering

methods will not be given: this has been extensively covered in the earlier Chapters.

2. APPLICATIONS TO VIRUS SYSTEMS

Total Intensity Light Scattering (TILS)

For smaller microbes like many viruses the simpler Rayleigh-Gans-Debye (RGD) theory is applicable and provided that $qR_g \ll 1$ (where q , R_g are the Bragg wave vector and the "radius of gyration" respectively) it is possible to use the TILS or "static"⁶ Zimm plot to obtain (i) the (weight average) molecular weight M_w , (ii) the radius of gyration, R_g , and (iii) the thermodynamic second virial coefficient, B (or A_2).

The static Zimm biaxial plot is based on the following relation:

$$Kc/R_\theta = (1/P(\theta)) [(1/M) + 2Bc + O(c^2)] \quad (3)$$

where c is the particle concentration (g/ml), θ is the scattering angle, K is an experimental constant which includes the square of the refractive index increment, R_θ is the Rayleigh excess ratio and $P(\theta)$ is the "form factor" which, in the limit of the scattering angle, $\theta \rightarrow 0$ takes the form

$$P(\theta) = 1 - (16\pi^2/3\lambda_0^2) R_g \sin^2(\theta/2) \quad (4)$$

Examples of Zimm plots applied to virus systems can be found for vaccinia virus (molecular weight, $M \sim 3 \times 10^9$)⁷, R17 virus ($M \sim 4 \times 10^6$)⁸ and tobacco mosaic virus, TMV ($M \sim 40 \times 10^6$)^{9,10}.

The radius of gyration from the static-Zimm plot, if used in conjunction with other techniques such as sedimentation analysis and the translational diffusion coefficient from QLS can be used to model the conformation of viruses and other macromolecular assemblies in terms of arrays of spherical particles or "bead models": this procedure has proved particularly useful for the modelling of bacteriophages (see, *e.g.*, refs 11, 12). Alternatively "whole body" or triaxial ellipsoid modelling can be employed, involving combinations of R_g , B (after allowance for charge effects) and the intrinsic viscosity¹³. If a specific conformation of the virus is assumed (*e.g.* a rod), alternative relations for $P(\theta)$ are available permitting for example mass per unit length estimations⁶: this has been applied, for example, to a study of the rod shape bacteriophage fd¹⁴.

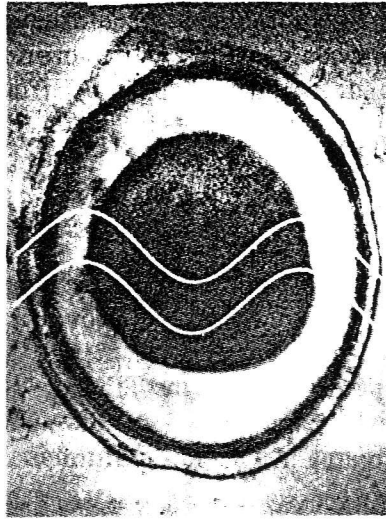


Figure 1. The maximum dimension of many microbes (in this example a spore from *B. cereus*) is of the same order as the wavelength of the incident (visible) radiation.

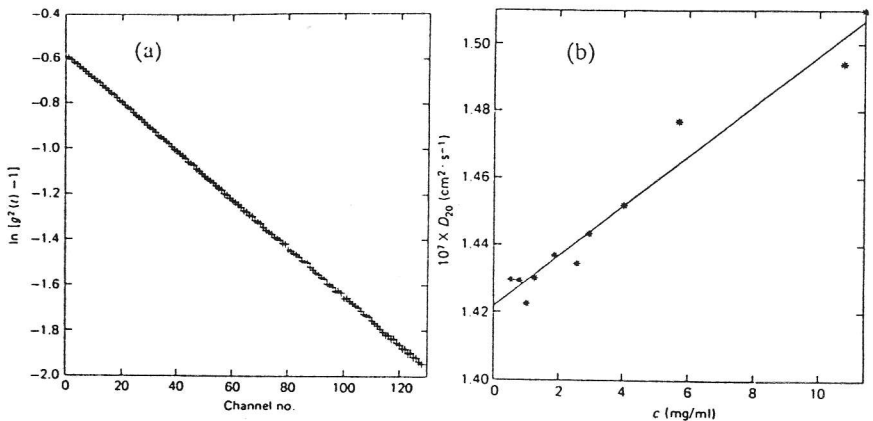


Figure 2. (a) Linear normalised autocorrelation decay plot for a quasi-spherical virus (TYMV). Channel number = delay time(τ)/sample time (τ_s). $\tau_s = 1.0 \mu\text{s}$; duration time = 60 s; scattering angle $\theta = 90^\circ$; temperature = 24.85°C; $c = 4.07 \text{ mg/ml}$; (b) Linear extrapolation of the apparent diffusion coefficient to zero concentration for TYMV. Reproduced, with permission, from ref. 19.

Quasi-elastic Light Scattering (QLS)

QLS contributions - in terms of the translational diffusion coefficient, D_T - to virology have been in four principal areas: (i) hydrodynamic rigid-bead modelling; (ii) flexible particle modelling; (iii) molecular weight measurement and (iv) for following the dynamics of assembly or swelling processes. As we have just mentioned, hydrodynamic modelling procedures based on QLS measurements are now well established (see, *e.g.* refs 2, 11, 12) and data capture and analysis¹⁵ is now relatively straightforward for quasi-spherical viruses such as tomato bushy stunt virus (TBSV), turnip yellow mosaic virus (TYMV) and many other plant viruses. For these quasi-sphericals, the simple single exponential term correlation equation, in terms of the normalised intensity autocorrelation function $g^{(2)}(\tau)$ - where τ is the delay time - is usually adequate¹⁶, provided that heterogeneity is not significant:

$$[g^{(2)}(\tau) - 1] = \exp(-D_T q^2 \tau) \quad (5)$$

The translational diffusion coefficient, D_T can thus be readily obtained from a plot of $\ln [g^{(2)}(\tau) - 1]$ versus τ (Fig. 2a). Measurements based on a single angle - usually a high one like 90° to minimise dust problems - are usually sufficient. If the system is polydisperse, D_T obtained from eq. 5 will be a z-average, and a measure of the polydispersity is usually given in the form of a "Polydispersity Factor", PF, *i.e.* the normalized z-average variance of the distribution of diffusion coefficients¹⁶. The D_T obtained from eq. 5 is usually corrected to standard solution conditions (water as solvent at a temperature of 20.0°C) and then extrapolated to zero concentration to give a parameter, $D_{T(20,w)}^0$ free of non-ideality effects¹⁷. As with macromolecules, for viruses a linear extrapolation is usually adequate (Fig 2b).

$$D_{T(20,w)} = D_{T(20,w)}^0 (1 + k_d) \quad (6)$$

where k_d is the concentration dependence diffusion coefficient parameter defined by¹⁸

$$k_d = 2BM - k_s - \bar{v} \quad (7)$$

and k_s is the sedimentation concentration dependence parameter and \bar{v} the partial specific volume. This equation explains why the concentration dependence of the diffusion coefficient is usually not as

severe compared with other hydrodynamic parameters (opposing effects on the RHS of eq. 7) and if k_s is known from a separate sedimentation velocity experiment, eqs. 6 and 7 provide an alternative route to eq. 3 for obtaining B, the thermodynamic second virial coefficient.

We have used QLS in this way to compare the gross morphology of TBSV variants¹⁹ and TYMV in various solvents²⁰. QLS translational diffusion coefficients have also been used *via* the Svedberg equation to evaluate the molecular weights of the bacteriophages type 5 adenovirus²¹, MS2²² and VS11²³, and also infectious pancreatic necrosis virus²⁴.

For rod-shape and other non-spheroidal viruses it is necessary to correct for rotational diffusion effects by measurement at several angles followed by a subsequent extrapolation to zero angle: a procedure which has yielded both D_T and the rotational diffusion coefficient D_R for tobacco mosaic virus (TMV)^{10,25,26} and bacteriophages T4B and T7²⁷. D_T and D_R values have also been recently obtained at a single angle (90°) from bimodal resolution using the "SIPP" algorithm²⁸.

Both extrapolations of $D_{T(20,W)}^0$ to zero concentration and zero angle can now be performed in a biaxial "dynamic" Zimm plot, and this procedure has been applied to microbial polysaccharides²⁹. For rod-like viruses anisotropy of D_T itself can be a problem³⁰. A further complication is one of particle flexibility, and Fujime and Maeda³¹ have considered this for filamentous fd virus. The effects of point (amino acid) mutations on the relative length and flexibility of fd has recently been considered³².

Comparison of data from TILS and QLS with other hydrodynamic data

The dangers - largely because of the serious errors resulting from even trace amounts of dust and other contaminating material - of using light scattering techniques in isolation for the characterisation of macromolecular solutions are widely appreciated. For solutions of viruses the situation is not as severe compared to the situation encountered when studying smaller macromolecules and assemblies^{4,33}, but independent confirmatory or complementary measurements - from for example analytical ultracentrifugation or

electron microscopy - are always useful. In general, agreement is good. Johnson and Brown¹⁰ in their article discussed the good agreement of molecular weight measurements from the QLS/Svedberg equation ($M \sim 40.8 \times 10^6$) with that from chemical analysis (39.4×10^6) and sedimentation equilibrium (41.6×10^6) for TMV. Similar good agreement has been obtained between TILS ($M \sim 14.6 \times 10^6$)¹⁴ and sedimentation equilibrium (14.2×10^6)³¹ for (wild-type) filamentous fd bacteriophage.

Another good example of agreement of results from laser light scattering with independent techniques is for the case of the quasi-spherical TYMV²⁰: the molecular weights evaluated from the translational diffusion coefficient and sedimentation coefficient *via* the Svedberg equation for four different solvents are in excellent agreement with those obtained independently from sedimentation equilibrium (Table 1a). Furthermore values for the second virial coefficient obtained from combination of the coefficient k_d obtained from the concentration dependence of the diffusion coefficient and k_s , the corresponding parameter from sedimentation velocity are in excellent agreement with the virial coefficient obtained from sedimentation equilibrium (Table 1b) and the hydrodynamic radii calculated from the translational diffusion coefficient are again in excellent agreement with the "thermodynamic" radii from the second thermodynamic virial coefficient from sedimentation equilibrium (Table 1c).

Despite their large size, it is possible to obtain preparations of virus solutions with very high monodispersities. This has made them highly suitable systems for testing experimentally the validity of theories representing the concentration dependence of the translational diffusion coefficient and related hydrodynamic parameters^{18,20}.

Analysis of dynamics of virus systems

Arguably the greatest value of laser light scattering methods - particularly QLS - in virology is for the analysis of the dynamics of self-assembly and related processes. We quote just two examples here. One (see, *e.g.*, Fig. 3a) is the analysis of the kinetics of head/tail assembly reactions for bacteriophages³⁴⁻³⁸; the second is the analysis of the effects of the removal of calcium ions on the dynamics of swelling of southern bean mosaic virus (SBMV), monitored by hydrodynamic diameters (Fig. 3b) and polydispersity

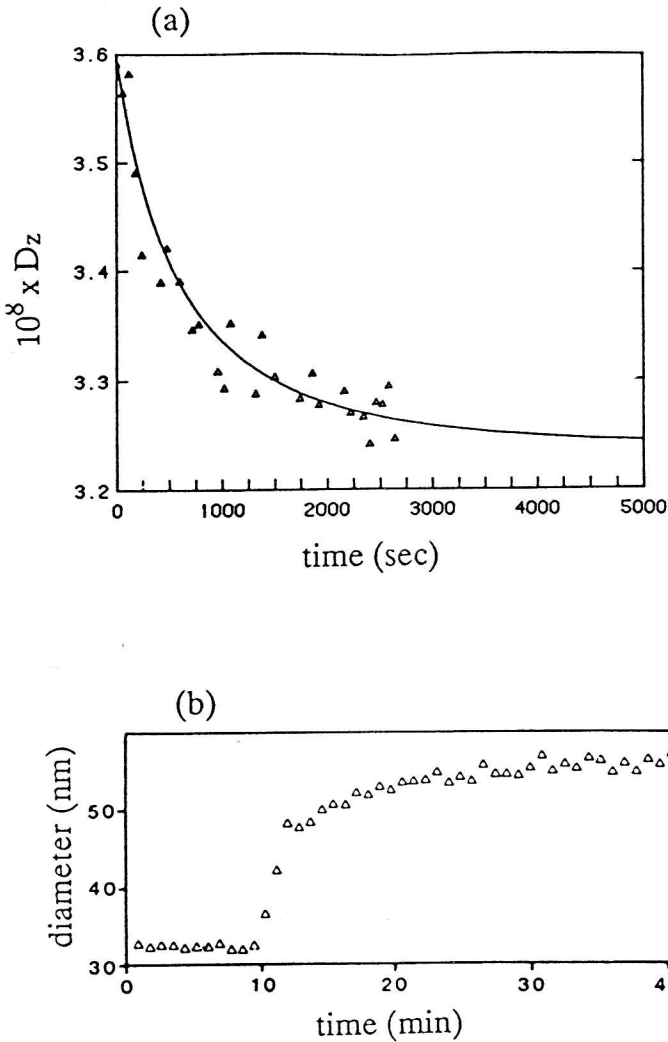


Figure 3. Following the dynamics of viral processes using QLS:
 (a) Head/tail association kinetics of T4D bacteriophage. Line fitted corresponds to an association constant, $k=7.9 \times 10^{-6} \text{ M}^{-1} \text{ s}^{-1}$. Reproduced with permission, from ref. 37.
 (b) Swelling of southern bean mosaic virus on removal of Ca^{++} ions. Reproduced with permission, from ref. 38.

Table 1. Physical data for TYMV: Agreement between QLS/sedimentation velocity and sedimentation equilibrium for various solvent pH and ionic strength conditions

(a) Molecular Weight

pH	I ^a	10 ⁻⁶ x M _w ^b (±0.05) g/mol	10 ⁻⁶ x M _w ^c (±0.2) g/mol	10 ⁻⁶ x M _w ^d (±0.2) g/mol
7.8	0.1	5.80	5.5	5.3
6.8	0.1	5.73	5.8	5.5
6.0	0.1	5.75	5.6	5.6
4.75	0.1	5.77	5.6	5.6
6.8	0.2	5.64	5.7	5.5

(b) Thermodynamic ('osmotic pressure') second virial coefficient, B

pH	I ^a	10 ⁶ x B ^e ±0.10 ml.mol.g ⁻²	10 ⁶ x B ^f ±0.4 ml.mol.g ⁻²
7.8	0.1	1.30	1.3
6.8	0.1	1.21	1.5
6.0	0.1	1.25	1.3
4.75	0.1	1.10	1.3
6.8	0.2	1.32	1.7

(c) Radii of equivalent spherical particle

pH	I ^a	r _H ^g (± 0.2) nm	r _B ^h (± 0.5) nm
7.8	0.1	15.1	16.3
6.8	0.1	15.1	15.8
6.0	0.1	15.2	15.9
4.75	0.1	15.5	15.4
6.8	0.2	14.9	16.1

(a) ionic strength; (b) from the sedimentation coefficient and the (QLS) translational diffusion coefficient via the Svedberg equation; (c) whole cell weight average from sedimentation equilibrium; (d) point weight average extrapolated to zero concentration (sedimentation equilibrium); (e) from k_D and k_S ; (f) from sedimentation equilibrium; (g) from the QLS translational diffusion coefficient; (h) from the (sedimentation equilibrium) value for B.

factors from QLS, in conjunction with total intensity measurements³⁹.

3. APPLICATIONS TO BACTERIAL AND OTHER CELLULAR MICROBIAL SYSTEMS

Both TILS and QLS have provided major inroads into our understanding of bacterial systems; perhaps most widely known is the application of QLS as a probe into the motility of bacteria and protozoa. However there has also been progress in other areas, such as the use of the total intensity method for modelling the structure - in terms of refractive index profiling - of isolated quasi-spherical bacterial spores and isolated marine micro-organisms, and also in the application of QLS for following the dynamics of suspensions of bacterial spore ensembles as a probe into their high resistance to thermal destruction; we will now survey some aspects of the progress in both these areas.

Total Intensity Light Scattering

With the larger microbes resonances in the angular scattered intensity profiles become significant - even at lower angles - and the Zimm plot and related methods become inapplicable. One ingenious solution was that of Morris *et al.*⁴⁰ who increased the wavelength of the incident radiation to the infra red, allowing application of the Zimm plot method to a particle whose hydrodynamic diameter was nearly a micron. This procedure has been applied⁴¹ to *Serratia marcescens* ($M \sim 0.7 \times 10^{11}$), *Escherichia coli* ($M \sim 1.0 \times 10^{11}$) and *Thiobacillus ferrooxidans* ($M \sim 1.6 \times 10^{11}$) and an example is given in Fig. 4. However in general the resonances in the angular scattered intensity envelopes have to be taken into account, and indeed provide potential information about internal structure - in terms of refractive index profiles - of micro-organisms.

RGD and Lorenz-Mie TILS representations

Refractive index profiling of microbes (in terms of *e.g.* average dimensions and refractive indices of concentric regions within the microbe - Fig. 5) is achieved by model fitting *i.e.* comparing the measured angular scattered intensity envelope (Fig. 6) with a theoretical profile based on a given model, and then iterating or refining this model until adequate agreement is obtained³. Thus this

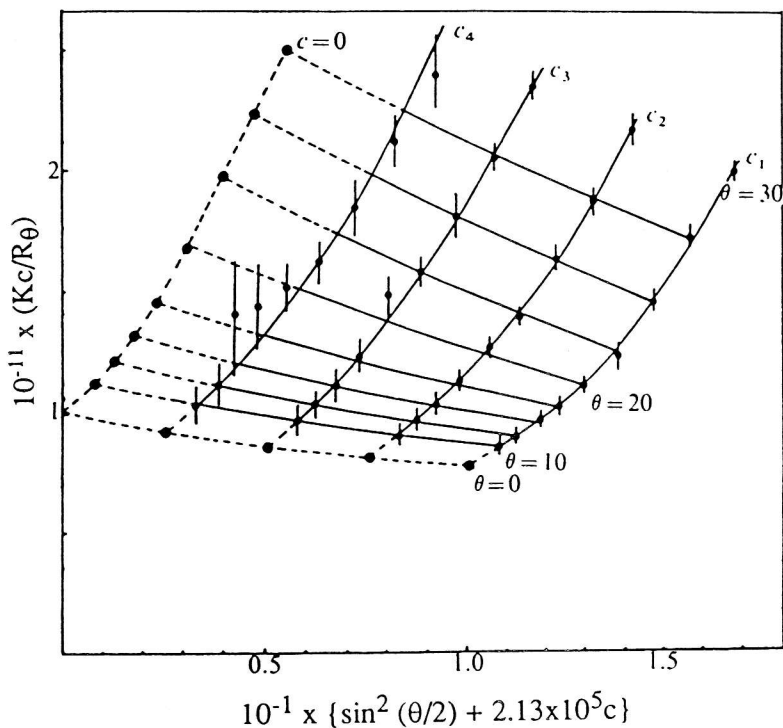


Figure 4. Zimm plot for a bacterium (*Serratia marcescens*) at $\lambda = 1.06 \mu\text{m}$. Stock concentration (c_1) = 0.47 g/ml. Reproduced, with permission, from ref. 40.

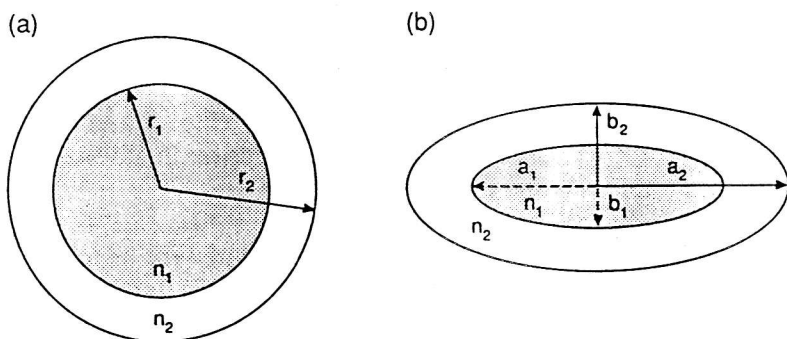


Figure 5. Refractive index profiling. (a) Coated sphere model: characterised by inner (or core) and outer (shell) radii, r_1 , r_2 and inner and outer refractive indices, n_1 , n_2 respectively (cf. Fig. 1); (b) Coated ellipsoid model: inner semi-axes a_1 , b_1 ; outer semi-axes a_2 , b_2 .

procedure differs from the Zimm / radius of gyration method which does not require any *a priori* assumed conformation⁶.

The RGD representations assume no change of phase or other distortions of the electric vector caused by the scattering particle: the phase differences between scattered waves from different points in a given particle are simply a function of position within that particle and not of the material of the particle⁶. [Representations are normally given for vertically polarised incident light since for horizontal or unpolarised light an extra term involving $\cos^2\theta$ can obscure these records^{3,42}].

Even for larger microbes the RGD theory can still give a reasonable representation of the scattered intensity profiles, provided that the refractive index difference between scatterer and medium is small (an example of this situation could be for a vegetative bacterial cell in aqueous suspension). A good illustration of the range of validities of RGD is given by Kerker (pp. 428-429 of ref. 6). For general RGD scatterers, the form factor $P(\theta)$ can be represented by the equation⁶:

$$P(\theta) = (1/V^2) \left| \int_V e^{i\delta} dV^2 \right| \quad (8)$$

where the integral is over the total volume, V of a particle whose volume elements produce a scattered phase δ at a common reference plane.

Explicit expressions for $P(\theta)$ have been worked out for a wide range of particle shapes: of particular use are the concentric (2 or 3 layered) sphere and coated ellipsoid models (Fig. 5 and refs 42,43) for modelling the refractive indices and approximate sizes of cell nuclei, protoplasm and membranes.

For many microbes however - particularly for bacterial spores which have a relatively high internal refractive index - the RGD approximation is not satisfied and account has to be taken of phase changes and other distortions of the electric field caused by the scattering microbe. The theory describing such scattering behaviour (Lorenz-Mie) is considerably more complicated and solutions for the intensity *versus* angle are only available for a very limited number of particle forms. Table 2⁴⁴⁻⁵³ lists those that are particularly relevant to situations involving micro-organisms. For particles with

spherical symmetry, the solution is summarised by the form, for vertically polarised incident light^{3,42}:

$$I(\theta) = \{I_0 / (qR)^2\} \left| \sum_{l=1}^{\infty} [{}^e B_l \tau_l(\cos \theta) + {}^m B_l \pi_l(\cos \theta)] \right|^2 \quad (9)$$

where $I(\theta)$ and I_0 are the intensities of the scattered and incident light respectively, R is the distance between the scattering particle and the reference plane or detector, ${}^e B_l$ and ${}^m B_l$ are the "electric" and "magnetic" scattering coefficients (involving Bessel functions) and τ_l and π_l angular functions involving Legendre type of polynomials.

Table 2. Particle types for which Lorenz-Mie solutions are available

Type	Ref.
Homogeneous sphere	44
Coated sphere	45
Multi-layered sphere	6
Spheres with continuously varying n	46,47
Homogeneous cylinders and ellipsoids	48
Coated ellipsoids	49,50,51
Homogeneous spheres with holes	52
Homogeneous spheres with projections	53

Asymmetry and Polydispersity

Despite the elegance of these theoretical advances, both RGD and Lorenz-Mie representations of the angular intensity envelopes have been difficult to apply for two fundamental reasons: (i) Random orientations of non-spherical scatterers: this tends to smooth out the resonances in the intensity envelope⁵¹. Fig. 6b illustrates this problem for a series of coated ellipsoids which could conceivably model bacterial spores; (ii) A further complication is of heterogeneity within a spore ensemble³ and the combined effects of both asymmetry and heterogeneity can lead to rather featureless angular intensity profiles as shown in Fig. 6c⁵⁴ for an ensemble of *B. subtilis* spores. It is still possible to infer some useful information from these type of curves: for example for antibiotic susceptibility testing⁵⁵ and in studies on the marine microbe *Chlorella*⁵⁶.

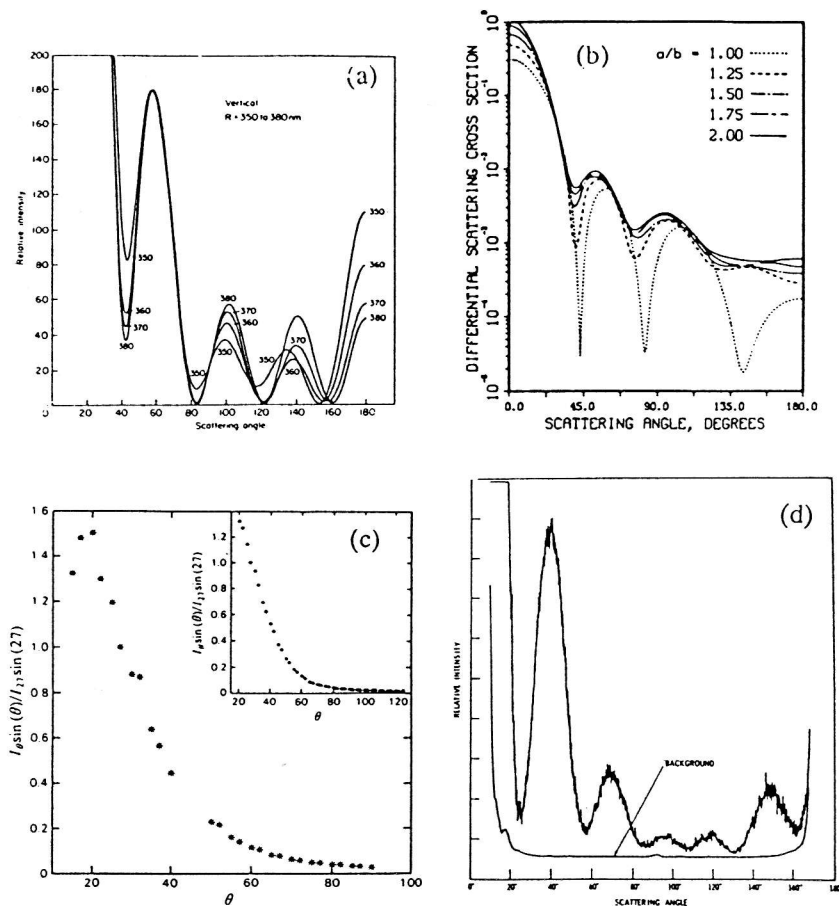


Figure 6. Angular scattered intensity envelopes from bacterial systems (vertically polarised incident radiation):

- (a) Theoretical TILS patterns for coated sphere models with varying radii. Reprinted, with permission, from ref. 3;
- (b) Theoretical TILS for randomly oriented ellipsoidal bacteria with varying aspect ratios. The dotted line corresponds to the normalized scattering intensity function against angle for a spherical particle showing strong structural features. As the ellipsoid aspect ratio is increased the structural features in the curve are smoothed out, making modelling approaching the impossible. Reprinted, with permission, from ref. 51;
- (c) Experimental TILS for a suspension of spores of *B. subtilis*. Reprinted, with permission, from ref. 54;
- (d) Experimental TILS, for a single isolated spore, suspended in air, of *B. sphaericus*. Reprinted, with permission, from ref. 57.

Single particle measurements

The "simple" solution - in principle - to asymmetry and heterogeneity is two fold. The first is to work with quasi-spherical bacterial spores. Although this greatly restricts the numbers of interesting systems that can be analysed there are some spores - such as from *B. sphaericus* - which have reasonable spherical symmetry. The second part of the solution is to record scattering intensity envelopes from isolated single spores. Wyatt and Phillips⁵⁷ successfully achieved this by using an aerosol technique to isolate single spores, giving successfully structural features which could be used for refractive index profiling (Fig. 6d). Suspending spores in air poses additional problems: for example, because of the relatively large refractive index difference between microbe and air, RGD theory is almost certainly not applicable, and more seriously the delicate osmotic balance between the interior and exterior of the microbe can be greatly disturbed - even for spores.

Instruments have been designed for multi-angle measurement of single particles in aqueous solution^{58,59}. Wyatt and Jackson⁵⁹ have indicated how such a device can be used to detect different phytoplankta from the characteristic scattered intensity envelopes. Ulanowski *et al.*^{60,61} have applied coated-sphere Lorenz-Mie theory to model the refractive index profiles of spores of *B. sphaericus* and basidiospores of *L. pyriforme* in water, and proposed this as a way of monitoring the water contents of spores. The technique is however currently limited to particles with spherical symmetry - because of the random orientation problem: application to the more interesting cases of ellipsoidal spores will require ways of providing constant orientation in the laser beam for a time long enough to get a sufficient signal/noise ratio across the angular scattered intensity envelope.

Flow cytometers

Similar in principle - although designed for a different purpose - are flow cytometers, which also facilitate light scattering measurements on single microbes^{62,63} and several commercial instruments are available (see, *e.g.* ref. 64). Light scattering detection from flow cells of suitable design are usually made at two scattering angles⁶³: although two is too few for the modelling of internal structures, it has been inferred that data of this type can permit the identification of microbial types⁶⁴.

Quasi-elastic light scattering of bacterial spores

QLS can also give useful information on bacterial spores, and moreover ensembles thereof. For quasi spherical spores, the single term exponential form of the autocorrelation function (eq. 5) gives a good representation of the data and as an example QLS has been used in parallel with turbidity measurements to monitor the possible changes in the gross morphology of *B. subtilis* spores⁵⁴ and *B. megaterium* spores⁶⁵ during germination - particularly during the early stages.

Such information has been used to help delineate between the various theories to explain the mechanisms responsible for the strong dehydration and heat resistance of bacterial spores. A similar application has been in the use of QLS in conjunction with electron microscopy⁶⁶ to show how culture growth temperature has an important effect on the resistance to thermal destruction (at 121°C). The effects of culture temperature on resistance to destruction by disinfectants has also been studied.

Chen *et al.*⁴³ have shown that "scaling" behaviour - *i.e.* superposition of plots of the autocorrelation function $g^{(2)}(\tau)$ plotted *versus* $q^2\tau$ for a range of angles - is a measure of the symmetry and homogeneity of a freely diffusing scattering particle. Non-scaling behaviour has been demonstrated for spores of *B. subtilis* (Fig 7a)⁵⁴ and *B. megaterium*⁶⁵ although germinated spores of *B. megaterium* do appear to scale better, possibly a measure of the decreased asymmetry and greater homogeneity of the germinated spores.

Microbial motility and chemotaxis

The most prolific application of QLS to microbiology has arguably been in this area. Besides being Brownian diffusers many microbes (flagellates, ciliates and bacteria) possess their own motility or "free translational motion"^{43,68} deriving from their own metabolism. QLS has provided a powerful non-destructive and non-invasive probe into this motility to study the velocity distributions of motile bacteria such as *E. coli*⁶⁸⁻⁷³, *Salmonella*^{61,74} and parasitic microorganisms such as *Trypanosoma brucei*^{75,76}. After neglecting contributions from "non-translational motion"^{77,74} the general equation describing

the intensity autocorrelation function $g^{(2)}(\tau)$ of motile microbes has been given as :

$$[g^{(2)}(\tau) - 1]^{1/2} = \int_0^{\infty} [\exp(i\mathbf{q}\cdot\mathbf{V})] P(\mathbf{V}) d^3\mathbf{V} \quad (10)$$

where \mathbf{V} is the velocity and $P(\mathbf{V})$ is the velocity distribution. For the relatively simple case of an isotropic distribution of velocities solution of the integral in eq. 10 gives an expression linking $g^{(2)}(\tau)$ with the root mean square velocity, the fraction of motile microorganisms and D_T . Scaling procedures similar to those for free Brownian diffusion (Fig. 7a) have been developed^{72,43} involving superposition of plots of $g^{(2)}(\tau)$ versus $q\tau$ (as opposed to $q^2\tau$ for free diffusion) for different angles as an assay for spherical symmetry and isotropicity of the scatterers. In this way for example Stock⁷⁴ has demonstrated scaling at low angles for *Salmonella typhimurium* (Fig. 7b). For typical non-scalers Chen and Hallett⁷⁸ have attempted a model to fit progressive rotational and helical movements. In recent work Wang and Chen⁷⁹ have studied the formation and propagation of bands of *E. coli* in the presence of oxygen and serine substrates, comparing two proposed formulisms for band formation.

4. DISCUSSION

Although this survey is by no means exhaustive it is hoped that it has given the Biochemist / Microbiologist an appreciation of the breadth of application to laser light scattering to microbial systems. Although it is probably fair to say that much of the attention over the last two decades has been in the application of dynamic light scattering or QLS, no less remarkable is the progress in static or total intensity light scattering for the analysis of single microbial particles in aqueous media.

Our own interest in this field is still principally in the application of laser light scattering as a probe into the heat resistance of bacterial spores: at the present time this is concerning itself with the detection of possible deleterious effects of the introduction of lux genes as a bioluminescent probe. The difficulties in applying QLS have been in terms of the inherent polydispersity of bacterial systems and also, if a dynamic process is being followed, variability in the rates at which individual spores germinate or are destroyed by chemical agents. To this end the value of combining QLS

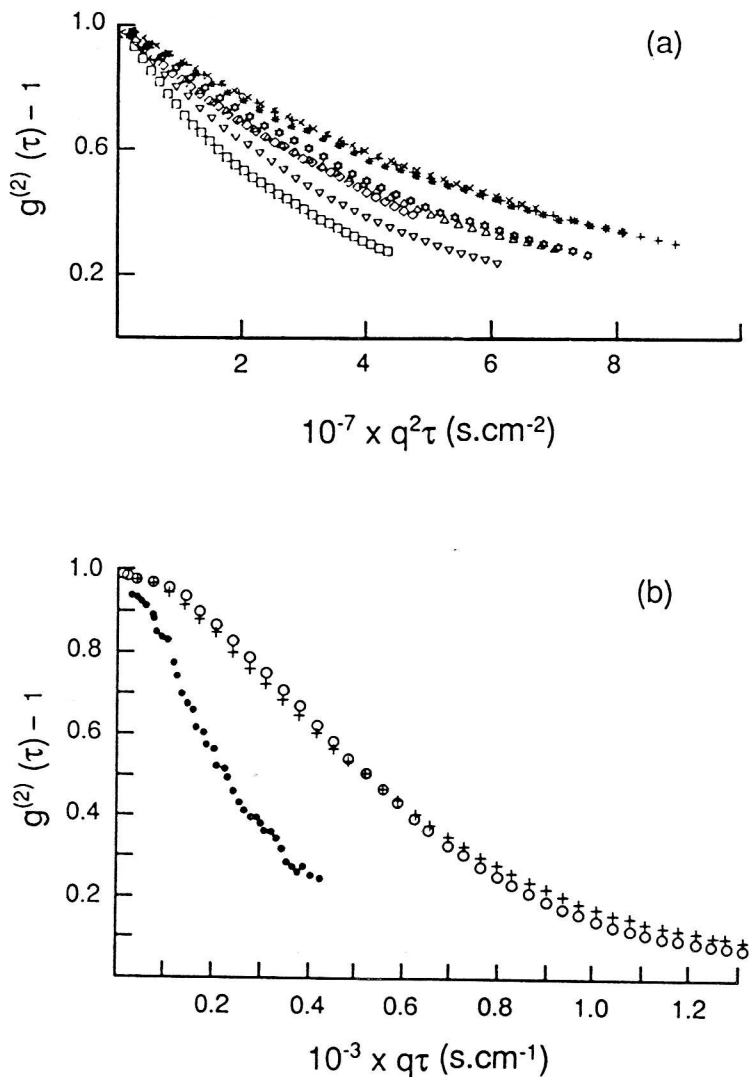


Figure 7. QLS scaling plots of bacterial systems:

(a) $q^2\tau$ scaling for spores of *B. megaterium* (from ref. 65);

(b) $q\tau$ scaling, for *E. coli* (Reprinted, with permission, from ref. 74).

The different symbols in each case correspond to different angles. In (a) no scaling is evident. In (b) scaling is evident only at low angles.

measurements on spore ensembles with measurements by TILS on single spores is clearly indicated. An important development in this area will occur when a method is developed to fix the orientation of individual non-spherically symmetric microbes in a laser beam to permit refractive index profiling of many more species than can currently be realistically studied.

ACKNOWLEDGEMENTS

My interest in light scattering of microbial systems arose during my collaboration with P. Johnson and I thank him for many valuable discussions. I am grateful also to A. Molina-Garcia for his valuable contributions to our work on tomato bushy stunt virus, fd bacteriophage and *Bacillus cereus* spores.

REFERENCES

1. S.E. Harding, *Biotech. & Appl. Biochem.*, 1986, 8, 489.
2. V.A. Bloomfield, *Ann. Rev. Biophys. Bioeng.*, 1981, 10, 421.
3. P.J. Wyatt, *Meth. Microbiol.*, 1973, 8, 183.
4. See, for example A.H. Sanders and D.S. Cannell in 'Light Scattering in Liquids and Macromolecular Solutions' (V. Degiorgio, M. Corti and M. Giglio eds.), pp. 173-182, Plenum, New York, 1980.
5. P.J. Wyatt, Chap. 3, this volume.
6. M. Kerker, 'The Scattering of Light and other Electromagnetic Radiation', Academic, New York, 1969.
7. R.J. Fiel, E.H. Mark and B.R. Munson, *Arch. Biochem. Biophys.*, 1970, 141, 547.
8. R.D. Camerini-Otero, PhD Thesis, New York University, 1973.
9. H. Boedtker and N.S. Simmons, *J. Amer. Chem. Soc.*, 1958, 80, 2550.
10. P. Johnson and W. Brown, Chap. 11, this volume.
11. J. Garcia de la Torre and V.A. Bloomfield, *Quart. Rev. Biophys.*, 1981, 14, 83.
12. J. Garcia de la Torre, in 'Dynamic Properties of Biomolecular Assemblies' (S.E. Harding and A.J. Rowe eds.), Chap. 1, Royal Society of Chemistry, Cambridge, 1989.
13. S.E. Harding, *Biophys. J.*, 1987, 51, 673.
14. S.A. Berkowitz and L.A. Day, *J. Mol. Biol.*, 1976, 102, 531.

15. V.A. Bloomfield and T.K. Lim in 'Methods in Enzymology' (C.H.W. Hirs and S.N. Timasheff eds.) Vol. 48 Pt. F, pp. 414-494, Academic, Fl., 1978.
16. P. Pusey in 'Photon Correlation and Light Beating Spectroscopy' (H.Z. Cummins and E.R. Pike eds.) pp 387-428, Plenum, New York, 1974.
17. C. Tanford, 'Physical Chemistry of Macromolecules', Chap. 6, Wiley and Sons, New York, 1961.
18. S.E. Harding and P. Johnson, *Biochem. J.*, 1985, 231, 543.
19. A.D. Molina-Garcia, S.E. Harding and R.S.S. Fraser, *Biopolymers*, 1990, 29, 1443.
20. S.E. Harding and P. Johnson, *Biochem. J.*, 1985, 231, 549.
21. C.J. Oliver, K.F. Shortridge and G. Belyavin, *Biochim. Biophys. Acta.*, 1976, 437, 589.
22. P. Nieuwenhuysen and J. Clauwaert, *Biopolymers*, 1978, 17, 2039.
23. Y. Sakaki, T. Maeda and Y. Oshima, *J. Biochem. (Tokyo)*, 1979, 85, 1205.
24. P. Dobos, R. Hallett, D.T.C. Kells, O. Sorensen and D. Rowe, *J. Virol.*, 1977, 22, 150.
25. J.C. Thomas and G.C. Fletcher, *Biopolymers*, 1978, 17, 2755.
26. Y. Sano, *J. Gen. Virol.*, 1987, 68, 2439.
27. P.C. Hopman, G. Koopmans and J. Greve, *Biopolymers*, 1980, 19, 1241.
28. A.A. Timachenko, N.B. Griko and I.N. Serdyuk, *Biopolymers*, 1990, 29, 303.
29. W. Burchard, Chap. 1, this volume.
30. J. Wilcoxon and J.M. Schurr, *Biopolymers*, 1983, 22, 849.
31. S. Fujime and T. Maeda, *Macromolecules*, 1985, 18, 191.
32. A.D. Molina-Garcia, S.E. Harding, F.G. Diaz, J.Garcia de la Torre, D. Rowitch and R.N. Perham (1991) mss. submitted.
33. R.E. Godfrey, P. Johnson and C.J. Stanley in 'Biomedical Applications of Laser Light Scattering' D.B. Sattelle, W.I. Lee and B.R. Ware eds.), pp 373-389, Elsevier, Amsterdam, 1982.
34. G.J. Baran and V.A. Bloomfield, *Biopolymers*, 1978, 17, 2015.
35. J.B. Welch and V.A. Bloomfield, *Biopolymers*, 1978, 17, 2001.
36. J.A. Benbasat and V.A. Bloomfield, *J. Mol. Biol.*, 1975, 95, 335.
37. J.A. Benbasat and V.A. Bloomfield, *Biochemistry*, 1981, 20, 5018.
38. B.V. Chernyak, *FEMS Microbiol. Lett.*, 1982, 13, 113.

39. M. Brisco, C. Haniff, R. Hull, T.M.A. Wilson and D.B. Sattelle, *Virology*, 1986, 148, 218.
40. V.J. Morris, H.J. Coles and B.R. Jennings, *Nature*, 1974, 249, 240.
41. H.J. Coles, B.R. Jennings and V.R. Morris, *Phys. Med. Biol.*, 1975, 20, 225.
42. P.J. Wyatt, *Appl. Optics*, 1968, 7, 1879.
43. S.-H. Chen, M. Holz and P. Tartaglia, *Appl. Opt.*, 1977, 16, 187.
44. G. Mie, *Ann. Physik.*, 1908, 25, 377; see also ref. 6 for a discussion on the appropriateness of whom should be credited with this theory.
45. A.L. Aden and M. Kerker, *J. Appl. Phys.*, 1951, 22, 1242.
46. P.J. Wyatt, *Phys. Rev.*, 1962, 127, 1837.
47. P.J. Wyatt, *Phys. Rev.*, 1964, 134, AB1.
48. S. Asano and M. Sato, *Appl. Opt.*, 1980, 19, 962.
49. P.W. Barber, PhD Thesis, Univ. California, Los Angeles, 1973.
50. P.W. Barber and H. Massoudi, *Aerosol. Sci. Med. Technol.*, 1982, 1, 303.
51. D.S. Wang, H.C.H. Chen, P.W. Barber and P.J. Wyatt, *Appl. Opt.*, 1979, 18, 2672.
52. P. Latimer, *Appl. Optics*, 1984, 23, 1844.
53. P. Latimer, *Appl. Optics*, 1984, 23, 442.
54. S.E. Harding and P. Johnson, *Biochem. J.*, 1984, 220, 117.
55. D.W.L. Hukins, J. Murray and P. Evans, *UV Spectrom. Group. Bull.*, 1980, 8, 18. For a critical review of methods, see also J. Kiehlbauch, J.M. Kendle, L.G. Carlson, F.D. Schoenknecht and J.J. Plorde, *Clinics in Lab. Med.*, 1989, 9, 319.
56. M.S. Quinby-Hunt, A.J. Hunt, K. Lofftus and D. Shapiro, *Limnol. Oceanog.*, 1989, 34, 1587.
57. P.J. Wyatt and D.T. Phillips, *J. Colloid Interface Sci.*, 1972, 39, 125.
58. I.K. Ludlow and P.H. Kaye, *J. Colloid Interface Sci.*, 1979, 69, 571.
59. P.J. Wyatt and C. Jackson, *Limnol. Oceanog.*, 1989, 34, 96.
60. Z.J. Ulanowski, I.K. Ludlow and W.M. Waites, *FEMS Microbiol Lett.*, 1987, 40, 229.
61. Z.J. Ulanowski, I.K. Ludlow and W.M. Waites, *Microbiol. Research*, 1989, 93, 28.
62. H.B. Steen and T. Lindmo, *Science*, 1979, 204, 403.
63. G. C. Salzman, in 'Cell Analysis' (N. Catsimpoolas ed.), Chap. 5, Plenum, New York, 1980.

64. R.W. Spinrad and J.F. Brown, *Appl. Optics*, 1986, 25, 1930.
65. S.E. Harding and P. Johnson, *J. Appl. Bacteriol.*, 1986, 60, 227.
66. A.D. Molina-Garcia, S.E. Harding, L. de Pieri, N. Jan and W.M. Waites, *Biochem. J.*, 1989, 263, 883.
67. G.B. Stock, *Biophys. J.*, 1976, 16, 535.
68. R. Nossal and S.-H. Chen, *Opt. Commun.*, 1972, 51, 117.
69. R. Nossal and S.-H. Chen, *Nature*, 1973, 244, 253.
70. D.W. Schaefer and B.J. Berne, *Biophys. J.*, 1975, 15, 785.
71. M. Holz and S.-H. Chen, *Appl. Opt.*, 1978, 17, 1930.
72. P.C. Wang and S.-H. Chen, *Biophys. J.*, 1981, 36, 203.
73. S.H. Chen and P.C. Wang in 'Biomedical Applications of Laser Light Scattering' (D.B. Sattelle, W.I. Lee and B.R. Ware eds.), pp 173-190, Elsevier, Amsterdam, 1982.
74. G.B. Stock, *Biophys. J.*, 1978, 22, 79.
75. R.J. Gilbert, R.A. Klein and P. Johnson, *Biochem. Pharmacol.*, 1983, 32, 3447.
76. R.A. Klein, *Biochem. Soc. Trans.*, 1984, 12, 629.
77. R. Nossal, S.H. Chen and C.C. Lai, *Opt. Commun.*, 1971, 4, 35.
78. S.H. Chen and F.R. Hallett, *Q. Rev. Biophys.*, 1982, 15, 131.
79. P.C. Wang and S.H. Chen, *Biophys. J.*, 1986, 49, 1205.